



HAL
open science

Kinetics of oxydation by scanning probe microscopy : a space-charge-limited model

Emmanuel Dubois, J.L. Bubendorff

► **To cite this version:**

Emmanuel Dubois, J.L. Bubendorff. Kinetics of oxydation by scanning probe microscopy : a space-charge-limited model. *Journal of Applied Physics*, 2000, 87, pp.8148-8154. 10.1063/1.373510 . hal-00158510

HAL Id: hal-00158510

<https://hal.science/hal-00158510v1>

Submitted on 20 Sep 2024

HAL is a multi-disciplinary open access archive for the deposit and dissemination of scientific research documents, whether they are published or not. The documents may come from teaching and research institutions in France or abroad, or from public or private research centers.

L'archive ouverte pluridisciplinaire **HAL**, est destinée au dépôt et à la diffusion de documents scientifiques de niveau recherche, publiés ou non, émanant des établissements d'enseignement et de recherche français ou étrangers, des laboratoires publics ou privés.

Kinetics of scanned probe oxidation: Space-charge limited growth

Emmanuel Dubois^{a)} and Jean-Luc Bubendorff

IEMN/ISEN, UMR CNRS 8520, Avenue Poincaré, Cité Scientifique, BP 69, 59652 Villeneuve d'Ascq, Cedex, France

(Received 23 July 1999; accepted for publication 9 February 2000)

This article proposes an enhanced oxidation model for scanning probe microscope (SPM) nanolithography that reproduces the power-of-time law reported for tip-induced anodic oxidation. It is shown that the space charge resulting from nonstoichiometric states strongly limits the oxidation rate. The direct relationship between the oxide thickness and time is provided by integration of the oxide rate equation. Measurements on SPM-induced oxides generated on a titanium surface are compared to theory. The predominant role of the space charge is corroborated by electrical measurements on oxide barriers that exhibit current fluctuations due to Coulombic effects. © 2000 American Institute of Physics. [S0021-8979(00)04310-3]

I. INTRODUCTION

Scanning probe microscopy (SPM) has recently demonstrated a strong potential in the field of nanolithography. In particular, SPM-induced nano-oxidation has been successfully used for patterning tunnel junctions¹ and field-effect devices² on thin metallic or SOI films, respectively. The strong activity developed around this lithography technique takes advantage of the simplicity to reach nanometer range and to visualize the corresponding patterns with the same equipment. Several contributions have reported on the mechanism and kinetics of SPM-based oxidation³⁻⁶ in order to get a better control and more detailed insight of this patterning method. However, none of them gives a complete and satisfactory explanation for the wide range of experimental data available in the literature. This article proposes an enhanced oxidation model for SPM nanolithography that reproduces the power-of-time law reported for tip-induced anodic oxidation.⁶ In Sec. II, existing models are first recalled and their deficiencies are outlined. In Sec. III, a new modeling approach accounting for space-charge limited growth is subsequently derived. It is shown that the space charge resulting from nonstoichiometric states strongly limits the oxidation rate. For the first time, the direct relationship between the oxide thickness and time is provided by integration of the oxide rate equation. In Sec. IV, measurements on SPM-induced oxides generated on a titanium surface are compared to theory. Finally, the predominant role of the space charge is corroborated by electrical measurements on oxide barriers that exhibit current fluctuations due to Coulombic effects.

II. EXISTING MODELS

A. Cabrera–Mott model

Recently, a modeling approach based on the Cabrera–Mott⁷ analysis of very thin oxide films has been published.³ Oxide growth under high electric field is described by ion migration at a rate given by

$$\frac{dh}{dt} = u \cdot \exp\left(\frac{h_1}{h}\right), \quad (1)$$

where h is the oxide thickness at time t , h_1 is a characteristic distance depending on the interfacial potential difference and u is a velocity function of temperature. The integration by parts of Eq. (1) is usually performed by neglecting higher terms in h/h_1 to give

$$u \cdot t = \left(\frac{h^2}{h_1}\right) \cdot \exp\left(\frac{-h_1}{h}\right). \quad (2)$$

It is subsequently assumed in Refs. 3 and 7 that the film thickness appearing in the pre-exponential term can be replaced by a limiting film thickness, h_L , beyond which the film ceases to grow. This is generally defined as the thickness at which one layer of atoms is added in 10^5 s so that $dh/dt = 10^{-13}$ cm s⁻¹. Using this assumption, Eq. (2) takes the so-called inverse logarithmic form

$$\frac{1}{h} = \frac{1}{h_1} \cdot \ln\left(\frac{h_L^2}{h_1 u t}\right). \quad (3)$$

It is worth noting that insertion of the solution Eq. (3) into the rate Eq. (1) gives

$$\frac{dh}{dt} = \frac{h_L^2}{h_1 t} \quad (4)$$

from which we obtain, by integration, the direct logarithmic form which obviously contravenes the inverse logarithmic [Eq. (3)] from which it is derived. The previous analysis shows that a careful inspection of the assumption made to integrate the rate equation reveals an inconsistent $h-t$ relationship. While the master rate equation remains valid, a more sophisticated mathematical treatment is necessary to correctly describe the anodic oxide growth. Nevertheless, no attempt to solve this problem is made in this work as the Cabrera–Mott rate equation needs additional ingredients to lead to a more comprehensive model as shown in the following.

^{a)}Electronic mail: dubois@isen.fr

B. Avouris–Hertel–Martel model

Experimental determination of the oxide growth rate has been performed in Ref. 5. The authors showed that the kinetics could not obey the Cabrera–Mott model because this theory predicts a rate constant proportional to $\exp(-h_1/h)$ while experiments clearly revealed that

$$\frac{dh}{dt} \propto \exp\left(-\frac{h}{h_c}\right), \quad (5)$$

where h_c is a characteristic decay thickness depending on the anodization voltage. The form of Eq. (5) is similar to the empirical relationship proposed by Massoud, *et al.*⁸ to explain the oxidation rate in the thin regime at high temperature in O₂ ambience. Large stress buildup during oxidation is invoked to explain the reduction of the oxidation kinetics. A strain relief mechanism due to the electric field is assumed to describe the dependence of h_c on the anodization voltage. Although a detailed discussion was provided in this article, no detailed derivation of the reaction kinetics was established to elucidate the empirical aspect of Eq. (5). Moreover, a recent analysis by Dagata *et al.*⁴ showed that the variations of the oxide density with pulse duration of the anodization voltage was incompatible with cumulative stress buildup.

C. Empirical power-of-time model

Systematic experiments on the oxide thickness dependence on voltage and tip speed (i.e., proportional of the inverse of time) have been conducted by Ley *et al.*⁶ Over a wide range of anodization voltages, tip speeds, and silicon substrates, the authors showed that the two-parameters empirical relation given by Eq. (6) gave a remarkable fit to the whole set of data,

$$h = \alpha_0 \cdot (U - U_{th}) \left(\frac{v_0}{v}\right)^\gamma \propto \alpha_0 \cdot (U - U_{th}) \left(\frac{t}{t_0}\right)^\gamma. \quad (6)$$

The threshold voltage U_{th} being known, α_0 and γ are the two relevant independent parameters. The oxidation time is inversely proportional to v , the tip speed. In the case of a silicon substrate, γ was found equal to 1/4 regardless of the type and level of doping. Despite a wide range of applicability of this simple empirical model over data available in the literature, no theoretical foundation was given to support the physical meaning of Eq. (6).

III. MODEL OF SPACE-CHARGE LIMITED SPM-INDUCED OXIDATION

A. Theory of oxide growth rate

It is now well accepted that the low activation found for SPM-induced oxidation is representative of anodic oxidation.^{3,4} Depending on the experimental conditions, both plasma oxidation⁹ and electrochemical anodic oxidation¹⁰ are known to produce a large amount of interface charges. Dagata *et al.*⁴ also outlined the role of a rapid buildup of space charge within the field-induced oxide during the initial stage of growth while rejecting the stress model introduced by Avouris *et al.*⁵ It will be shown that the presence of this space charge is responsible for the drastic reduction of the

growth rate as the oxidation proceeds. After an oxide layer has grown, fixed oxide charges are generated close to the bulk/oxide interface. For instance, Beck *et al.*⁹ attributes the presence of these charges to the initial high rate of oxidation that prevents a complete saturation of broken bonds at the bulk/oxide interface resulting in nonstoichiometric states. As outlined by Wolters and Zegers-van Duynhoven,¹¹ the variation of this space charge in the oxide is governed by a trapping–detrapping mechanism. For large charge densities (e.g., $>10^{12}$ cm⁻²), Coulomb interactions between trapped charges and newly incorporated charges must be taken into account to calculate the trapping rate. On this basis, the integration of the trapping rate equation yields

$$N = \frac{1}{s} \cdot \ln\left(1 + \frac{sN_0\sigma}{q} \cdot \int_0^t J \cdot dt'\right) = \frac{1}{s} \cdot \ln\left(1 + \frac{Q}{Q_0}\right), \quad (7)$$

where s is the surface occupied by a trap. N is the areal density of traps and N_0 is the maximum areal density of trap sites, σ is the effective trap capture cross section and $Q_0 = q/sN_0\sigma$. Q is the integrated areal density of charge obtained from the incoming flux of oxyanions. It corresponds to the charge brought by oxyanions that have crossed the oxide layer at time t

$$Q = \int_0^t J \cdot dt'. \quad (8)$$

Q can be simply calculated from C_{ox} the concentration of oxygen in the oxide, $Q = zqC_{ox}h$ where h is the oxide thickness, q the electronic charge, and z the number of electronic charge per ion. Considering that the trapped charges density N is a consequence of the total oxyanion charge (e.g., OH⁻) transported to the oxide/bulk interface, the space charge comes from nonstoichiometric states and is of opposite sign (e.g., positive for silicon or titanium). Therefore, a positive areal charge density is assumed confined close to the bulk/oxide interface at a distance h_0 . This charge N induces a distortion of the electric field that significantly influences the transport of oxydizing agents in the oxide layer. The initial electric field between the bulk/oxide interface and the positive charge density N is decreased by the following amount:

$$\xi_{bias} \rightarrow \xi_{bias} - \frac{qN}{\epsilon} \cdot \frac{h-h_0}{h} = \xi_{bias} - \frac{q}{s\epsilon} \cdot \frac{h-h_0}{h} \cdot \ln\left(1 + \frac{zqC_{ox}h}{Q_0}\right), \quad (9)$$

where ϵ is the oxide dielectric constant and $\xi_{bias} = -(U_{tip} - U_{bulk})/h = U_{bias}/h$ is the external field imposed by the tip and substrate voltages. The potential and electric field distribution are depicted in Fig. 1. It is assumed hereafter that the flux of oxyanions through the oxide layer is totally controlled by the region where the electric field is decreased by the presence of the space charge. The ionic transport equation that describes oxide growth rate is given by⁷

$$\frac{dh}{dt} = u_0 \cdot \exp\left(-\frac{W}{kT}\right) \cdot \sinh\left(\frac{qa\xi}{kT}\right), \quad (10)$$

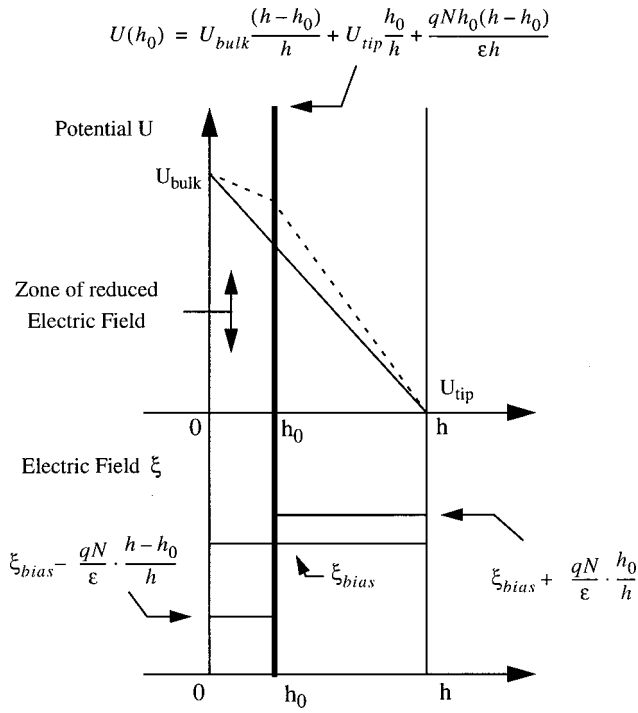


FIG. 1. Potential and electric field distortion induced by the presence of an areal charge density $qN = q/s \cdot \ln(1 + zqC_{ox}h/Q_0)$ located at h_0 . The oxide/bulk interface located at 0 and h represents the thickness of the growing oxide.

where u_0 is a constant velocity, W is the energy barrier that an ion has to overcome to move to the next interstitial sites located at a distance $2a$. ξ is the electric field including the distortion induced by the space charge. Only the exponential term with a positive argument is relevant when the transport of oxyanions from the ambient to the bulk/oxide interface is considered. Accounting for the previous remark, insertion of Eq. (9) into Relation (10) yields

$$\frac{dh}{dt} = u_0 \cdot \exp\left(-\frac{W}{kT}\right) \cdot \exp\left\{\frac{zqa}{kT} \cdot \frac{U_{bias}}{h} - \delta \cdot \frac{(h-h_0)}{h} \cdot \ln\left(1 + \frac{zqC_{ox}h}{Q_0}\right)\right\}, \quad (11)$$

where δ is a dimensionless parameter equal to $q^2a/kTs\epsilon$. It is worth noting that as the centroid of the space charge layer is located very close to the bulk/oxide interface, $(h-h_0)/h$ rapidly converges to unity. Thus, a simplified expression for the rate of oxide growth can be derived using $h_b = Q_0/zqC_{ox} = 1/sN_0\sigma zC_{ox}$ and $h_a = zqaU_{bias}/kT$

$$\frac{dh}{dt} = u_0 \cdot \exp\left(-\frac{W}{kT}\right) \cdot \exp\left\{\frac{h_a}{h} - \delta \ln\left(1 + \frac{h}{h_b}\right)\right\}. \quad (12)$$

Typical values of the capture cross section σ are around 10^{-13} cm^{-2} ,¹² one order of magnitude for N_0 is 10^{13} cm^{-2} (Ref. 10) and s can be set to first order equal to σ . From the previous parameter values, a rough estimation for δ gives $\sim 2-6$ for titanium or silicon ($C_{ox} \sim 4 \cdot 10^{22} \text{ cm}^{-3}$ for SiO_2 , $\sim 4.5 \cdot 10^{22} \text{ cm}^{-3}$ for TiO_2). This value is difficult to ascertain from individual parameter extractions. However, the above estimation appears reasonable as it will be shown in

the following that $1/\delta$ may be related to the exponent of the power law between the oxide thickness and time. For instance, it was experimentally observed that SiO_2 thickness varies with time as $h \propto t^{1/2}$ (Ref. 13) or as $h \propto t^{1/4}$ (Refs. 6 and 14). In the following section, other measurements performed on TiO_2 reveal $h \propto t^{1/5}$. Taking $a \sim 0.15 \text{ nm}$,⁶ $h_a = 5.81$. U_{bias} appears as a linear function of the anodization bias (h_a expressed in nanometers). From the same set of parameters, h_b gives $\sim 0.002 \text{ nm}$, a value extremely small that allows to further simplify Eq. (12) since $h/h_b \gg 1$

$$\frac{dh}{dt} = u_0 \cdot \exp\left(-\frac{W}{kT}\right) \cdot \exp\left(\frac{h_a}{h}\right) \left(\frac{h}{h_b}\right)^{-\delta}. \quad (13)$$

B. Extraction of the power-of-time law

The integration of Eq. (13) remains a difficult task but can be performed assuming that δ is an integer. This prerequisite does not correspond to any physical quantification process but simply reflects a mathematical constraint to obtain a tractable relationship between h and t . It will be shown that the above condition is not a severe constraint as δ usually lies in the 2–6 range. The Eq. (13) may be recast under its integrated form

$$u_0 \cdot \exp\left(-\frac{W}{kT}\right) \cdot t = \int_0^h \exp\left(\frac{-h_a}{h'}\right) \left(\frac{h'}{h_b}\right)^\delta dh'. \quad (14)$$

Successive integration by parts of the right-hand side (rhs) of Eq. (14) gives

$$\int_0^h \exp\left(\frac{-h_a}{h'}\right) \left(\frac{h'}{h_b}\right)^\delta dh' = \frac{h_a^{\delta+1}}{h_b^\delta} \left\{ \frac{(-1)^{\delta+1}}{(\delta+1)!} \cdot Ei\left(\frac{h_a}{h}\right) + \sum_{i=0}^{\delta} (-1)^i \cdot \frac{(\delta-i)!}{(\delta+1)!} \cdot \left(\frac{h}{h_a}\right)^{\delta+1-i} \cdot \exp\left(-\frac{h_a}{h}\right) \right\}, \quad (15)$$

where $Ei(h_a/h) = \int_0^h e^{-h_a/h'} / h' dh'$ is a variant of the exponential integral function. It can be verified that this expression rapidly decays for $h < h_a$, a condition that is easily satisfied for common anodization voltages. Recalling that $h_a \sim 5.81 U_{bias}$, a typical example for $U_{bias} = 6 \text{ V}$ gives $h_a \sim 35 \text{ nm}$, while the corresponding oxide thickness h reported in the literature lies generally one decade below.^{15,16} Therefore, Eq. (15) may be simplified to give

$$\int_0^h \exp\left(\frac{-h_a}{h'}\right) \left(\frac{h'}{h_b}\right)^\delta dh' = \sum_{i=0}^{\delta} (-1)^i \cdot \frac{(\delta-i)!}{(\delta+1)!} \cdot h \cdot \left(\frac{h}{h_b}\right)^\delta \left(\frac{h_a}{h}\right)^i \cdot \exp\left(-\frac{h_a}{h}\right). \quad (16)$$

Finally, considering that $h \gg h_b$ (typ. $h_b = 0.002 \text{ nm}$), the summation over δ appearing in the rhs of Eq. (16) can be

approximated by its first term that largely dominates the following ones. Accounting for these considerations, the integration of Eq. (14) is well approximated by

$$h = h_b \left(\frac{t}{t_0} \right)^{1/(\delta+1)}, \quad (17)$$

where t_0 is a voltage-dependent time constant equal to

$$t_0 = \frac{h_b \cdot \exp\left(-\frac{h_a}{h}\right)}{(\delta+1) \cdot u_0 \exp\left(-\frac{w}{kT}\right)} = \frac{h_b \cdot \exp\left(-\frac{zqa}{kT} \cdot \frac{U_{\text{bias}}}{h}\right)}{(\delta+1) \cdot u_0 \exp\left(-\frac{w}{kT}\right)}. \quad (18)$$

In summary, the incorporation of a space charge submitted to Coulomb repulsion leads to a power-of-time law for oxide grown by SPM anodization. The above derivation is consistent with experimental observations made on silicon^{6,4} and titanium (this work). A physical significance may also be given to the time constant t_0 . Snow and Campbell¹⁷ have measured a voltage-dependent threshold time τ_{th} necessary to get a 0.3 nm oxide bump on SiO₂. They found that $\tau_{th} \propto \exp(-U_{\text{bias}}/U_0)$. Considering that h_{min} is the minimum detectable oxide thickness, the corresponding threshold time expressed according to Eqs. (17) and (18) exhibits the same consistent behavior with the anodization voltage

$$\tau_{th} = t_0 \cdot \left(\frac{h_{\text{min}}}{h_b} \right)^{\delta+1} \propto \exp\left(-\frac{zqa}{kT} \cdot \frac{U_{\text{bias}}}{h}\right). \quad (19)$$

The proposed model is based on the presence of a space charge due to nonstoichiometric states located close to the bulk/oxide interface. The main assumption in the model derivation is the occurrence of mutual Coulomb repulsions between traps and the control of the ionic transport by the region of lowest electric field. As outlined in Ref. 11, these assumptions are commonly used to treat transport phenomena in dielectrics. The presence of a large trap density during the formation of the very first oxide monolayers is questionable and depends on the presence of a native oxide. However, the onset of tip-induced anodization is characterized by the fastest growth rate that results in a large amount of defects. As soon as an oxide protusion becomes detectable (~ 1 nm), the oxidation process may be considered in a regime where the present model fully applies.

IV. EXPERIMENTS AND MODEL VALIDATION

The experiments were conducted with a Digital Instrument Nanoscope III microscope in tapping mode on a fresh 25 nm thick titanium layer deposited on a SiO₂/Si substrate by e-gun evaporation. The relative humidity level was kept in 50%-70% range, a condition that assures the presence of sufficient oxidizing agents (e.g., O⁻, OH⁻) contained in the absorbed layer of water. No perceptible change in oxide growth was observed under this humidity condition consistently with previous reports.^{18,19}

The experimental procedure can be divided into two distinct phases corresponding to the oxidation process by itself and to the subsequent imaging step needed to observe the oxidized patterns: During the oxidation phase, the atomic

force microscope (AFM) tip is kept at fixed location in the X–Y plane parallel to the titanium surface. In order to generate an oxide dot under the tip, a positive voltage pulse is applied to the substrate during a time varying between 5 ms and 50 s. The feedback loop is enabled and the setpoint is chosen to obtain an amplitude of vibration of 8 nm at a frequency around 330 kHz in tapping mode. Using this experimental setup, the position of the tip in the Z direction perpendicular to the interface is permanently adjusted by the feedback loop of the AFM. A tip coated with a 10 nm thick layer of Pt is used to prevent its oxidation. For each voltage/time couple, 25 different oxide dots are formed to get a valuable statistical representation of the measured oxide heights. Each step is controlled by a lithography program executed by the control computer. During the imaging phase, the AFM is used in the conventional scanning mode to generate the surface topography line by line.

It is worth noting that the measured oxide height from the AFM image does not correspond to the oxide thickness because the titanium layer is consumed by the oxidation process. Given the molar volume of Ti and TiO₂ (10.6 and 26.6 cm³, respectively), the expansion factor is 2.5 which corresponds to a 1.5 nm measured oxide height for each nanometer of consumed Ti. As a consequence, the total oxide thickness is obtained by multiplying the measured oxide height by a factor 1.667. The last correction holds only in the case of stoichiometric TiO₂, a situation that is theoretically not expected to hold in the case of anodic oxides. However, previous experiments conducted on a silicon surface have shown that this condition is fulfilled within a few percent.¹⁸

Figure 2 shows a series of AFM images corresponding to oxide dots fabricated at a voltage of 10 V for different pulse durations. These images illustrate the excellent reproducibility obtained under these operating conditions. Figure 3 represents the variations of the oxide thickness as a function of time for the three different voltage amplitudes. This plot shows that data are well fitted by a power-of-time law of the form $h \propto t^{1/5}$. This functional behavior is even better illustrated when h is plotted versus $(t/t_0)^{1/(\delta+1)}$ in Fig. 4. A straight line, obtained for the complete set of data, validates the applicability of the theory describing oxidation as a process strongly influenced by the buildup of a nonstoichiometric space charge. Finally, Fig. 5 gives the same $h-t$ set of data with a log–log scale. From this representation, the threshold time for a 1 nm oxide bump may be determined, 0.08, 1.5, and 40 ms for voltages of 6, 8, and 10 V, respectively. Several authors have pointed out the presence of a threshold voltage under which oxidation of silicon is not possible or drastically reduced. This threshold voltage depends on the type (*n* or *p*) and level of doping.^{6,18} One possible explanation of this effect lies in the relative magnitude of the density and capture cross sections of trapping sites when the doping type and the concentration vary.^{10,12} Consistently with these observations, variations on the trapping efficiency contribute to the modulation of h_b , which in turn, determine the magnitude of the time threshold in Eq. (19).

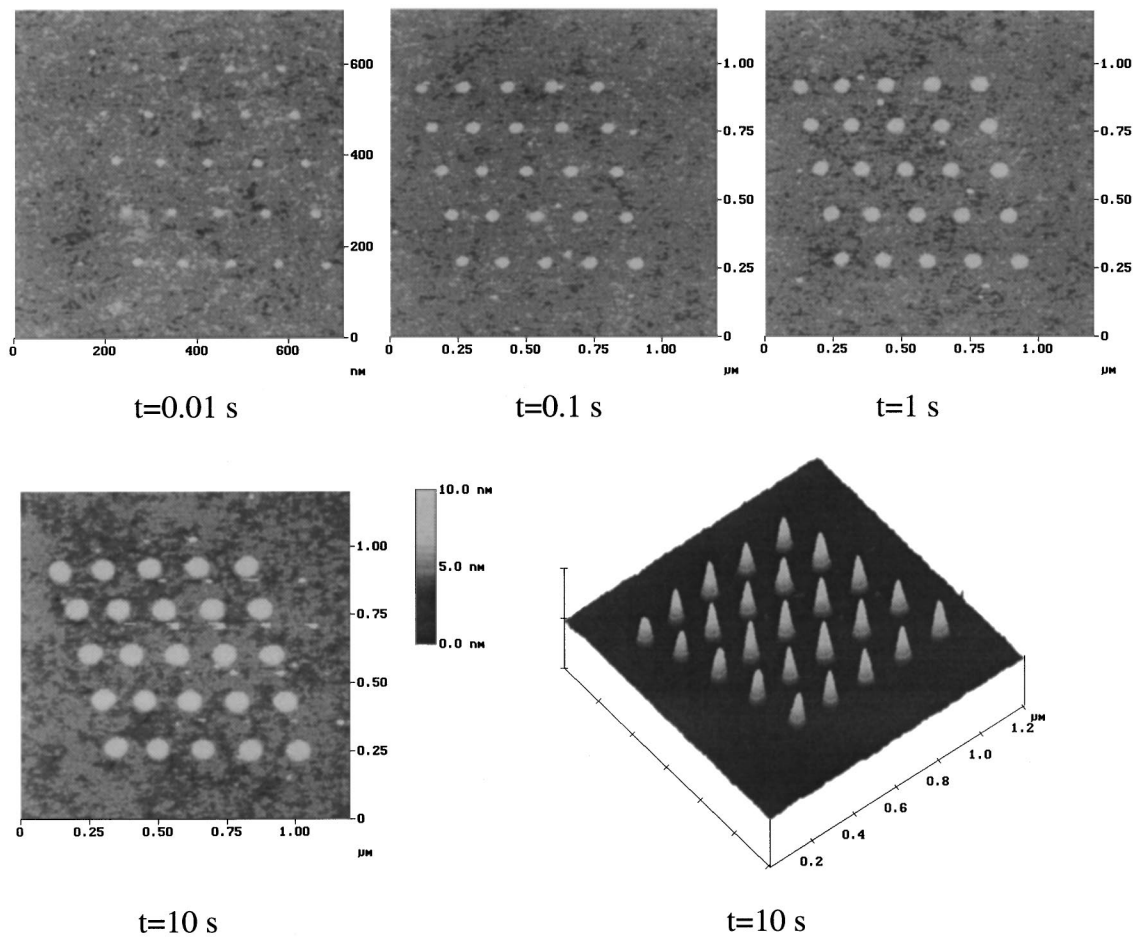


FIG. 2. AFM view of arrays of 25 oxide dots obtained after anodization induced by the tip of an AFM in tapping mode. The amplitude of the voltage pulse is 10 V and its duration varies from 10 ms to 10 s. Oscillation amplitude of the cantilever is 8 nm at a frequency around 330 kHz.

V. ELECTRICAL CHARACTERIZATION OF SPM ANODIC OXIDE

As outlined in Sec. III that reports on the modeling of SPM-induced anodization, the incorporation of space charge is related to the presence of nonstoichiometric traps due incomplete bonds saturation during the very fast initial stage of oxidation. It has been shown that Coulomb interactions must

be taken into account to properly evaluate the traps density [Eq. (7)]. In the present section, it is shown that the electron transport through TiO_2 barriers is severely affected by trapping and detrapping events governed by the same kind of Coulomb interactions that also determines the kinetics of oxide growth. In order to illustrate this point, SPM-induced oxide barriers have been fabricated on a thin Ti film²⁰⁻²² as

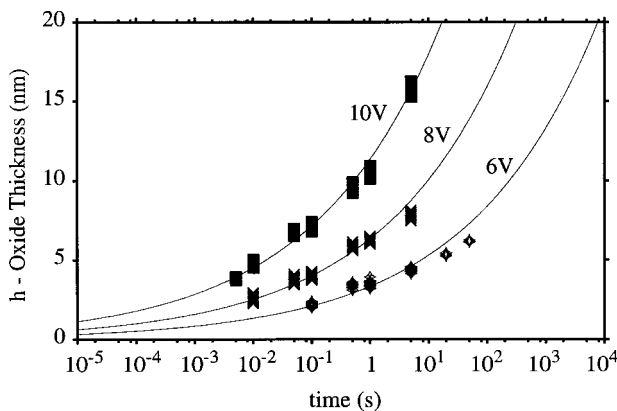


FIG. 3. Oxide thickness as a function of time for three different anodization voltages (6, 8, and 10 V). The surface is a 25 nm thick layer of titanium deposited on a Si/SiO₂ substrate.

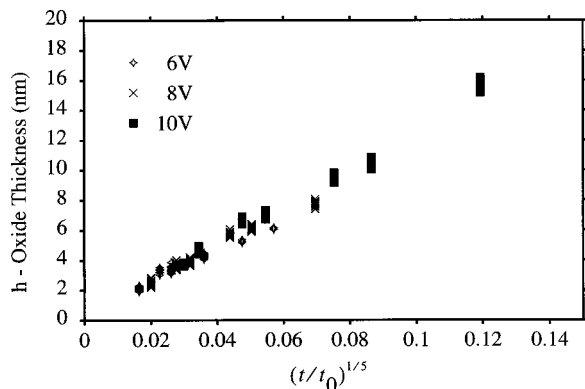


FIG. 4. Oxide thickness as a function of $(t/t_0)^{1/5}$. Data corresponding to three different anodization voltage (6, 8, and 10 V) are perfectly aligned. This representation validates the power-of-time law deduced from the kinetics of oxide growth.

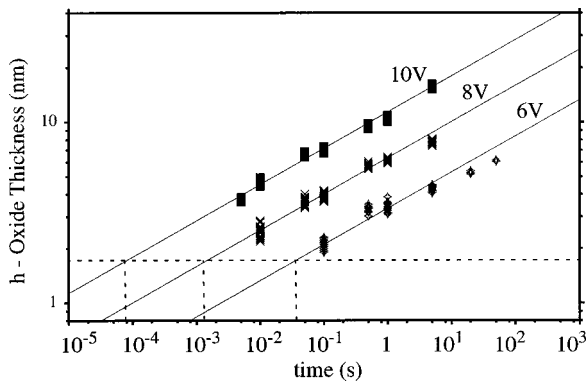


FIG. 5. Oxide thickness as a function of time for three different anodization voltages (6, 8, and 10 V). Threshold time for a 1 nm oxide bump is indicated: 0.08, 1.5, and 40 ms for voltages of 6, 8, and 10 V, respectively. Accounting for the amount of Ti consumed by the oxidation process, a 1 nm oxide height corresponds to a 1.667 nm oxide thickness.

shown in Fig. 6. The electrical characterization of these insulating barriers has been performed by measuring the corresponding current variations with time and for typical applied voltages ranging from -1 to 1 V. Special care has been devoted to the measurement setup to obtain a reduced noise level in low currents conditions (guarding techniques). Typical current versus time variations are reported in Fig. 7. Large current fluctuations are observed, similar to those observed in random telegraph signals (RTS) on small geometry metal-oxide-simiconductor field effect transistors (MOSFETs).²³⁻²⁶ The RTS, characterized by discrete change of drain current in MOSFETs, is governed by a trapping/

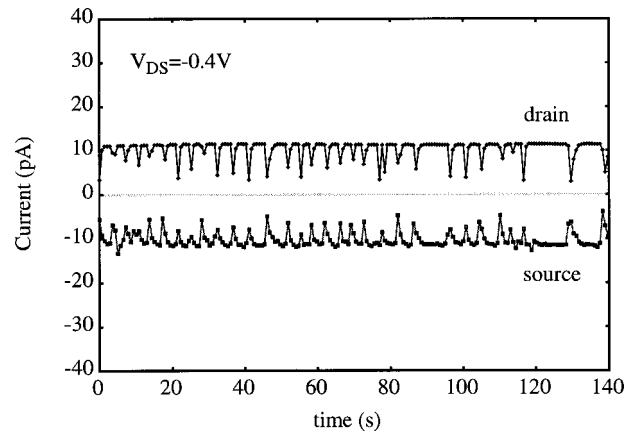


FIG. 7. Current vs time characteristic at a fixed source/drain voltage $V_{DS} = -0.4$ V. Fluctuations are related to a trapping/detrapping mechanism via individual nonstoichiometric traps.

detrapping process associated to individual defects near the SiO_2/Si interface.²⁴ The so-called Coulomb blockade involves a change in free energy by the transfer of an elementary charge between capacitor electrodes (of capacitance C). At room temperature, this is for extremely small capacitors that the charging energy $E = e^2/2C$ becomes sufficiently large to block another electron from transferring. As outlined by Schulz,²⁵ a trap center may be viewed as an extremely small capacitance that makes possible the existence of large Coulomb barriers. The influence of such Coulomb interactions explains single-electron trapping by individual traps that can result in RTS. It is now well accepted that both slow and fast traps can be involved in RTS. The time scale over which slow oxide traps are active is in the $1-100$ s range,²⁴ while fast interface traps are characterized by average capture and emission times in the $0.01-1$ s range.^{24,26} Figure 7 shows that the observed current fluctuations take place over a $1-3$ s time scale. A faster rate of current change is also possible but has not been resolved by a relatively long integration time related to the measurement equipment.

VI. CONCLUSION

In summary, we have proposed an enhanced model of oxidation under high electric field that includes the influence of a space charge due to nonstoichiometric traps at the oxide/bulk interface. Results for oxidation of titanium give an excellent fit to the power-of-time law. The model also corroborates similar results on silicon and explains the variations of the exponent δ with space-charge density ($h = t^{1/(\delta+1)}$). The voltage-dependent threshold time has also been deduced, consistently with other experiments carried out on silicon. It has been shown that the electron transport through TiO_2 barriers is severely affected by trapping and detrapping events governed by the same kind of Coulomb interactions that also determines the kinetics of oxide growth. From the present study, we conclude that the presence of traps and Coulombic interactions severely limits the applicability of direct SPM-oxidation for the fabrication of single-electron devices as the characteristics (location, energy level, type) of these traps can hardly be controlled.

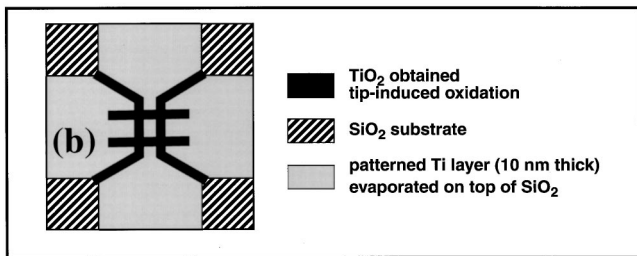
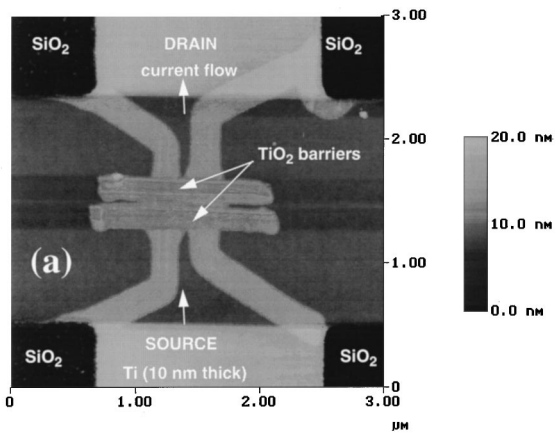


FIG. 6. (a) AFM image showing the direct formation of oxide barriers on a thin Ti film (10 nm) and (b) schematic view identifying the different materials: First a thin Ti layer was deposited and patterned using electron beam lithography. AFM-based lithography was subsequently applied to form TiO_2 barriers. Figure 7 reports on the current flowing through these barriers.

- ¹K. Matsumoto, M. Ishii, and K. Segawa, *J. Vac. Sci. Technol. B* **14**, 1331 (1996).
- ²P. M. Campbell, E. S. Snow, and P. J. McMarr, *Appl. Phys. Lett.* **66**, 1388 (1995).
- ³D. Stiévenard, P. A. Fontaine, and E. Dubois, *Appl. Phys. Lett.* **70**, 3272 (1997).
- ⁴J. A. Dagata, T. Inoue, J. Itoh, K. Matsumoto, and H. Yokoyama, *J. Appl. Phys.* **84**, 6891 (1998).
- ⁵P. Avouris, T. Hertel, and R. Martel, *Appl. Phys. Lett.* **71**, 285 (1997).
- ⁶L. Ley, T. Teuschler, K. Mahr, S. Miyazaki, and M. Hundhausen, *J. Vac. Sci. Technol. B* **14**, 2845 (1996).
- ⁷N. Cabrera and N. F. Mott, *Rep. Prog. Phys.* **12**, 163 (1948).
- ⁸H. Z. Massoud, J. D. Plummer, and E. A. Irene, *J. Electrochem. Soc.* **132**, 2685 (1985).
- ⁹R. B. Beck, M. Patyra, J. Ruzillo, and A. Jakubowski, *Thin Solid Films* **67**, 261 (1980).
- ¹⁰A. H. M. Kamal, S. Nomura, and T. Endoh, *J. Electrochem. Soc.* **141**, 2227 (1994).
- ¹¹D. R. Wolters and A. T. A. Zegers-van Duynhoven, *J. Appl. Phys.* **65**, 5126 (1989).
- ¹²W. D. Eades and R. M. Swanson, *J. Appl. Phys.* **58**, 4267 (1985).
- ¹³T. Hattori, Y. Ejiri, and K. Saito, and M. Yasutake, *J. Vac. Sci. Technol. A* **12**, 2586 (1994).
- ¹⁴T. Teuschler, K. Mahr, S. Miyazaki, M. Hundhausen, and L. Ley, *Appl. Phys. Lett.* **67**, 3144 (1995).
- ¹⁵R. Garcia, M. Calleja, and F. Perez-Murano, *Appl. Phys. Lett.* **72**, 2295 (1998).
- ¹⁶E. Dubois and J. L. Bubendorff, *Solid-State Electron.* **43**, 1085 (1999).
- ¹⁷E. S. Snow and P. M. Campbell, *Appl. Phys. Lett.* **64**, 1932 (1994).
- ¹⁸P. A. Fontaine, E. Dubois, and D. Stiévenard, *J. Appl. Phys.* **84**, 1776 (1998).
- ¹⁹H. Sugimura, T. Uchida, N. Kitamura, and H. Masuhara, *Appl. Phys. Lett.* **63**, 1288 (1993).
- ²⁰K. Matsumoto, *Proc. IEEE* **85**, 612 (1997).
- ²¹K. Matsumoto, Y. Gotoh, J. Shirakashi, T. Maeda, and J. S. Harris, *Tech. Dig. Int. Electron Devices Meet.* 155 (1997).
- ²²K. Matsumoto, Y. Gotoh, J. Shirakashi, T. Maeda, J. A. Dagata, and J. S. Harris, *Tech. Dig. Int. Electron Devices Meet.* 449 (1998).
- ²³A. Ohata, A. Toriumi, M. Iwase, and K. Natori, *J. Appl. Phys.* **68**, 200 (1990).
- ²⁴M. H. Tsai, H. Muto, and T. P. Ma, *Appl. Phys. Lett.* **61**, 1691 (1992).
- ²⁵M. Schulz, *J. Appl. Phys.* **74**, 2649 (1993).
- ²⁶S. T. Martin, G. P. Li, E. Worley, and J. White, *Appl. Phys. Lett.* **67**, 2860 (1995).